ELSEVIER

Mechanics of Materials 20 (1995) 291–303

MECHANICS OF MATERIALS

Viscoelastic analysis of mismatch stresses in ceramic matrix composites under high-temperature neutron irradiation ⋆

A. El-Azab, N.M. Ghoniem

Mechanical, Aerospace and Nuclear Engineering Department, 46-147G Eng. IV, University of California, Los Angeles, Los Angeles, California 90024, USA

Received 31 August 1993; revised version received 23 August 1994

Abstract

Fiber-reinforced ceramic matrix composites, such as SiC–SiC, are proposed for structural applications in future fusion energy systems. In a fusion nuclear reactor environment time-dependent inelastic effects are induced by irradiation and hence mismatch stresses are expected to change in time. The time evolution of the internal mismatch stresses in ceramic fiber composites under high-temperature neutron irradiation is presented, with application to SiC–SiC composite structures. The effects of thermal creep, irradiation-induced creep and dimensional changes on the build-up and relaxation of the interface pressure and residual stresses in fibers and matrix are investigated. Residual stresses are determined as functions of temperature and neutron exposure time. It is shown that initial mismatch stresses are relaxed within hours because of irradiation creep. It is also demonstrated that fibers with low density, such as Nicalon, will debond from the matrix due to excessive irradiation-induced densification.

Keywords: Viscoelasticity; Ceramics; Ceramic composites; Residual stresses; High temperature; Creep

1. Introduction

In fiber-reinforced ceramic matrix composites, mismatch stresses have a strong influence on the mechanical behavior of these materials. Mismatch stresses in fiber composites originate during manufacturing and processing because of two basic effects: phase transformations during consolidation and cooling from the fabrication temperatures. The pressure at the fiber–matrix interface plays a crucial role in the load transfer between the fiber and the matrix, both under normal loading of the composite and during failure. Composite failure theories (e.g., those developed by Aveston et al., 1971; Aveston and Kelly, 1973; Budiansky et al., 1986) emphasized the effects of mismatch stresses on the fracture strength of composites. Expressions for the optimal mismatch strains required to maximize the fracture strength of a ceramic matrix composite has been developed (Budiansky et al., 1986). Other authors, however, recognized the effects of the residual axial stress in fibers on fiber bridging of matrix cracks and fiber debonding both under pull-out and push down conditions (Sigl and Evans, 1989; Hutchinson and Jensen, 1990; Liang and Hutchinson, 1993; Gao et al., 1988). The high-temperature creep rates and creep resistance of composite materials are directly influenced by the internal mismatch stresses in the composite phases. These stresses drive a com-

⋆ This material is based upon work supported by the U.S. Department of Energy under award number DE-FG03-91ER54115 at UCLA.

SSDI 0167-6636(95)00009-7

plex load transfer process between the fiber and matrix, which is important in shear-lag theories of composite creep (Pachalis et al., 1990; Kelly and Street, 1972a,b).

Recently, silicon carbide (SiC) has been proposed as a structural material for first wall and blanket components in fusion nuclear power reactors (Najmabadi et al., 1994). Selection of SiC for this purpose is primarily based on its low activation characteristics under neutron irradiation. Monolithic SiC has a toughness of $K_{IC} \sim 4$ MPa $m^{1/2}$, which is at least 20 times lower than other candidate structural materials (e.g. steels). Cracks are expected to propagate in a brittle fashion, leading to catastrophic failures. In addition, the notch sensitivity of monolithic SiC makes fusion structural components vulnerable to impact loads which are likely to be induced by plasma disruptions. Based on these factors, it is proposed to use SiC which is fiber reinforced, and hence achieve higher fracture resistance. In a fusion reactor, structural materials must have the capability to operate reliably under constant neutron irradiation and at high temperatures for long periods. Under these conditions, inelastic effects such as thermal creep, irradiation-induced creep and irradiation-induced dimensional changes are important in determining the component lifetime.

Irradiation-induced dimensional changes and the irradiation creep contribute to the build-up and relaxation of the mismatch stresses. Dimensional changes under irradiation can be in the form of volumetric swelling, e.g. dislocation loop swelling, void swelling and gas bubble swelling, or shrinkage by densification. Nucleation and growth of such micro structures are driven by the intense atomic displacements and gas production which result from nuclear reactions between neutrons and the matrix atoms. Dimensional changes under irradiation can also be associated with irradiation-driven phase transitions, such as amorphization or recrystallization. Irradiation creep is kinetically possible once the material is subjected to combined irradiation and stress fields. However, irradiation-induced creep and dimensional changes are time-dependent, and can be significantly different in different composite phases. Therefore, both phenomena are expected to cause time evolution of the residual internal stress fields in the composite phases under high temperature neutron irradiation, while the material is in service.

In this paper, we study the effects of irradiation creep and swelling on the build-up and relaxation of the residual mismatch stresses in ceramic matrix composites under fusion conditions. Thermal creep is also considered. The developed model treats both composite phases (fiber and matrix) as linear viscoelastic solids. This allows the elastic–viscoelastic correspondence principle, along with the method of Laplace transform, to be used for obtaining the time history of internal stresses from the elastic solution. The elastic solution is first developed and is based on the concentric cylinder model of composites. The temperature of the composite system is assumed to be independent of time. The SiC–SiC composite system, proposed recently for a conceptual fusion reactor study (Najmabadi et al., 1994) is taken as a case study. Experimental data on irradiation-induced dimensional changes and irradiation creep for SiC–SiC composites are used (El-Azab and Ghoniem, 1994). Results for the interface pressure at the fiber–matrix interface and for the axial stresses in fiber and matrix are presented as functions of temperature and neutron exposure time.

2. Elastic solution

The concentric cylinder model depicted in Fig. 1 is taken to represent a composite reinforced with a volume fraction, $f = (R_f/R_0)^2$, of aligned continuous fibers. The mismatch consists of a thermal strain component, $\alpha\Delta T$, and a swelling (*or shrinkage*) strain

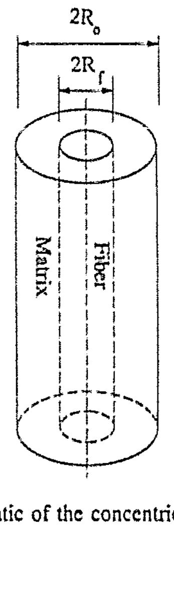

Fig. 1. Schematic of the concentric cylinder model.

component, ϵ^s, for both fibers and matrix. The matrix is β-SiC which is produced by CVD or CVI processes. Two types of SiC fibers are considered; Nicalon and SCS-6 fibers. Unlike Nicalon fibers and CVD-SiC matrix, the SCS-6 SiC fibers will be treated as transversely isotropic materials which exhibit different swelling response in the axial and transverse directions. The model, therefore, is developed for transversely isotropic fibers embedded in an isotropic matrix. The case of isotropic fibers is treated as a special case of the developed solution. The concentric cylinder is considered to be infinitely long and free of any external forces. In this case, the stress field and its time-evolution within the composite cylinder is completely determined by mismatch strains, both thermal and swelling, and irradiation and thermal creep. As stated, this is a Lamé stress problem for which the stresses in the fiber and matrix are given in terms of the interface pressure q by the following relations:

$$\begin{aligned}
\sigma_r^f &= q, \\
\sigma_\theta^f &= q, \\
\sigma_r^m &= \frac{q}{(1-f)}\left[\left(\frac{R_f}{r}\right)^2 - f\right], \\
\sigma_\theta^m &= \frac{-q}{(1-f)}\left[\left(\frac{R_f}{r}\right)^2 + f\right],
\end{aligned} \quad (1)$$

where the superscripts "f" and "m" refer to the fiber and matrix, respectively, r is the distance from the fiber center, and R_f is the fiber radius. Elasticity solutions for this system are well developed, and the corresponding strains are given by:

$$\begin{aligned}
\epsilon_r^f &= \epsilon_{tr}^f + \frac{(1-\nu_f)q}{E_{tr}} - \frac{\nu_f \sigma_z^f}{E_{ax}}, \\
\epsilon_\theta^f &= \epsilon_r^f, \\
\epsilon_z^f &= \epsilon_{ax}^f + \frac{\sigma_z^f}{E_{ax}} - \frac{2\nu_f q}{E_{tr}}, \\
\epsilon_r^m &= \epsilon_{in}^m + \frac{1}{E_m}\left(\frac{q}{(1-f)}\left[\left(\frac{R_f}{r}\right)^2 (1+\nu_m) - f(1-\nu_m)\right] - \nu_m \sigma_z^m\right), \\
\epsilon_\theta^m &= \epsilon_{in}^m - \frac{1}{E_m}\left(\frac{q}{(1-f)}\left[\left(\frac{R_f}{r}\right)^2 (1+\nu_m) + f(1-\nu_m)\right] - \nu_m \sigma_z^m\right), \\
\epsilon_z^m &= \epsilon_{in}^m + \frac{1}{E_m}\left(\sigma_z^m + \frac{2\nu_m f q}{(1-f)}\right),
\end{aligned} \quad (2)$$

where E_{tr} and E_{ax} are the transverse and axial Young's moduli of the fiber, and ν_f is the fiber Poisson's ratio, which is taken to be the same for strain coupling between the three normal directions. E_m and ν_m have the same definitions for the matrix. ϵ_{tr}^f, and ϵ_{ax}^f are the transverse and axial inelastic strain components in the fiber, respectively, and ϵ_{in}^m is the inelastic strain in the matrix. These quantities are defined by:

$$\begin{aligned}
\epsilon_{tr}^f &= \int_{T_0}^{T} \alpha_{tr}(T')\,dT' + \epsilon_{tr}^s, \\
\epsilon_{ax}^f &= \int_{T_0}^{T} \alpha_{ax}(T')\,dT' + \epsilon_{ax}^s, \\
\epsilon_{in}^m &= \int_{T_0}^{T} \alpha_m(T')\,dT' + \epsilon_m^s,
\end{aligned} \quad (3)$$

where the α's are the coefficients of thermal expansion and the subscripts "tr" and "ax" refer to transverse and axial directions of the fiber, respectively, and "m" refers to the matrix. $\epsilon_{tr,ax,m}^s$ are swelling strain components in the fiber and matrix. Expressions for these strains are given in Section 3.

In deriving the solution given by Eqs. (1) and (2), continuity of the radial stress across the interface is imposed. As shown in these two equations, the stress and strain fields in the composite cylinder are completely determined by three unknowns; the interface pressure, q, the axial stress in the fiber, σ_z^f and the axial stress in the matrix, σ_z^m. These stress quantities can be determined in terms of imposed inelastic strains, by applying the following conditions:

(i) The axial self-equilibrium condition for the composite cylinder, which is written as:

$$f\sigma_z^f + (1-f)\sigma_z^m = 0. \quad (4)$$

(ii) The kinematic boundary conditions, given by:

$$\epsilon_z^{\mathrm{f}} = \epsilon_z^{\mathrm{m}},$$
$$\epsilon_\theta^{\mathrm{f}}(R_{\mathrm{f}}) = \epsilon_\theta^{\mathrm{m}}(R_{\mathrm{f}}), \tag{5}$$

the first of which is the condition of compatibility (no relative sliding) along the axial direction, while the second is the condition of continuity of the radial displacement across the interface.

Equilibrium in the axial direction is satisfied by axial stresses which are independent of the radial coordinate and are uniform along the axial direction. The three conditions given by Eqs. (4) and (5) are used to obtain the three unknowns q, σ_z^{f} and σ_z^{m}. By enforcing these conditions, the following expressions are obtained for the unknown stresses:

$$q = E_{\mathrm{tr}} E_{\mathrm{m}} (1-f) \left(\frac{b_2 \Delta\epsilon_{\mathrm{tr}} - b_1 \Delta\epsilon_{\mathrm{ax}}}{a_1 b_2 - a_2 b_1} \right),$$
$$\sigma_z^{\mathrm{f}} = E_{\mathrm{tr}} E_{\mathrm{m}} (1-f) \left(\frac{-a_2 \Delta\epsilon_{\mathrm{tr}} + a_1 \Delta\epsilon_{\mathrm{ax}}}{a_1 b_2 - a_2 b_1} \right),$$
$$\sigma_z^{\mathrm{m}} = \left(\frac{-f}{1-f} \right) \sigma_z^{\mathrm{f}} \tag{6}$$

where

$$a_1 = (1-f)(1-\nu_{\mathrm{f}}) E_{\mathrm{m}} + E_{\mathrm{tr}} \left[(1+\nu_{\mathrm{m}}) + f(1-\nu_{\mathrm{m}}) \right],$$
$$b_1 = -\left(\frac{E_{\mathrm{tr}}}{E_{\mathrm{ax}}} \right) \left[(1-f)\nu_{\mathrm{f}} E_{\mathrm{m}} - f \nu_{\mathrm{m}} E_{\mathrm{ax}} \right],$$
$$a_2 = -2 \left[(1-f)\nu_{\mathrm{f}} E_{\mathrm{m}} + f \nu_{\mathrm{m}} E_{\mathrm{tr}} \right],$$
$$b_2 = \left(\frac{E_{\mathrm{tr}}}{E_{\mathrm{ax}}} \right) \left[(1-f) E_{\mathrm{m}} + f E_{\mathrm{ax}} \right],$$
$$\Delta\epsilon_{\mathrm{tr}} = \epsilon_{\mathrm{in}}^{\mathrm{m}} - \epsilon_{\mathrm{tr}}^{\mathrm{f}},$$
$$\Delta\epsilon_{\mathrm{ax}} = \epsilon_{\mathrm{in}}^{\mathrm{m}} - \epsilon_{\mathrm{ax}}^{\mathrm{f}}. \tag{7}$$

Before presenting the viscoelastic solution, correlations for irradiation effects in SiC matrix and SiC fibers are presented and expressions for the total creep and relaxation functions under high-temperature neutron irradiation are formulated. The irradiation data on creep and dimensional changes are presented in terms of the neutron flux, temperature, and irradiation time, for the conceptual fusion reactor study ARIES IV first wall conditions (El-Azab and Ghoniem, 1994).

3. Irradiation effects in CVD-SiC and SiC fibers

3.1. CVD-SiC matrix

Irradiation-induced linear dimensional changes in the CVD-SiC matrix consist of two components: a dislocation loop swelling component and a helium swelling component. The percent linear loop swelling is given empirically by:

$$\epsilon^{\ell} = \left[1.05 - 10^{-3}(T - 273) \right] \times \left[1 - \exp\left(-t/t_0 \right) \right], \tag{8}$$

where T is the temperature in K, t is the irradiation time, and t_0 is the time constant for saturation of loop swelling, which depends on the operating neutron flux. This formula for loop swelling is valid only below 1000°C. For ARIES IV first wall conditions, the saturation time constant t_0 is estimated to be 30 minutes. The helium swelling component is given by the following phenomenological equation (El-Azab and Ghoniem, 1994):

$$\epsilon^{\mathrm{He}} = \left(\frac{1}{12\pi} \right)^{1/2} \left(\frac{kT}{2\gamma} \frac{f_{\mathrm{He}} G_{\mathrm{He}} t}{N^{1/3}} \right)^{1.5} = C_{\mathrm{SiC}}(T) t^{1.5}, \tag{9}$$

in which k is the Boltzmann constant, G_{He} is the helium generation rate, f_{He} is the fraction of helium retained in the material, γ is the surface energy, and N is the helium bubble density. For the ARIES IV Tokamak reactor:

$$G_{\mathrm{He}} = 2.898 \times 10^{19}\ \mathrm{atoms/m^3\ s},$$
$$f_{\mathrm{He}} = 0.2,$$
$$N = 5.18 \times 10^{17} \exp\left(\frac{2.63 \times 10^{-19}}{kT} \right)\ \mathrm{m^{-3}}.$$

The numerical constants in this Arrhenius representation of the bubble density are estimated by fitting the irradiation data of Price (1973). It is important to mention here that the time scale for helium swelling is much longer than that for loop swelling in SiC. Helium swelling occurs over a time span of years under fusion conditions. The total swelling strain in the matrix, ϵ_m^s, is given by:

$$\epsilon_m^s = \epsilon^\ell + \epsilon^{He}. \tag{10}$$

The irradiation creep compliance, which is the creep strain per unit stress, of CVD-SiC matrix is given by (Price, 1977):

$$J_m^{irr} = K\phi t, \tag{11}$$

where the creep constant $K = 10^{-25}$ (MPa·n·cm^{-2})$^{-1}$, $\phi = 1.65 \times 10^{15}$ n · cm^{-2} s^{-1}, is the operating neutron flux, and t is the time in seconds.

3.2. SCS-6 fibers

SCS-6 fibers are produced by chemical vapor deposition of SiC on a carbon core. In a typical SCS-6 fiber, the carbon core volume fraction, f_c is 0.08. El-Azab and Ghoniem (1994) have developed expressions for the axial and transverse swelling strains and irradiation creep compliance for SCS-6 fiber under neutron irradiation. These expressions are based on irradiation effect data of SiC, and are written for the swelling strains as:

$$\epsilon_{tr}^s = (1 - f_c)\epsilon_m^s, \quad \epsilon_{ax}^s = \epsilon_m^s \tag{12}$$

and for the irradiation creep compliance as:

$$J_{tr}^{irr} = J_m^{irr}, \quad J_{ax}^{irr} = J_m^{irr}/(1 - f_c). \tag{13}$$

As known, SCS-6 fibers have comparatively large diameters (~140 microns) which limits their use in ceramic matrix composite systems since the composite fracture strength decreases as the fiber radius increases (Evans, 1990, 1991). Also these fibers cannot be easily woven. Because the fiber radius is irrelevant in the present analysis, SCS-6 fibers are considered since this kind of fiber, which is ~92% β-SiC, is desirable from the irradiation stand point.

Eq. (12) suggests that the transverse swelling rate for SCS-6 fibers is smaller than that of the matrix. This equation was derived based on a purely geometrical argument (El-Azab and Ghoniem, 1994). In the present study, however, the swelling of such fibers will be parametrically represented in terms of the matrix swelling. The reason this approach is followed here is, as will be shown later, that it is necessary that the fiber swelling rate must be higher than that of the matrix in order to maintain a compressive interfacial stress. Limits for differential swelling factors can then be chosen for optimum composite response. Differential swelling, in particular helium-type swelling, can be directly related to relative concentrations of helium-producing atomic species in fiber and matrix. Boron doping, for example, can help obtain the desired limits for the differential helium swelling parameters.

3.3. Nicalon fibers

Nicalon fibers undergo a densification process under neutron irradiation (Okamura et al., 1985). This densification is partly due to recrystallization, where β-SiC crystallites form. Under fusion neutron irradiation, the time-dependent linear shrinkage associated with densification is given by (El-Azab and Ghoniem, 1994):

$$\epsilon^{shr} = -\frac{a}{3}\frac{t^2}{\rho_0 + at^2}, \tag{14}$$

where t (seconds) is the irradiation time, ρ_0 (g cm^{-3}) is the initial density of Nicalon fibers, and $a = 6.2\,(\phi/\Phi_0)^2$, $\Phi_0 = 10^{21}$ n·cm^{-2}. Shrinkage of Nicalon fibers is estimated to saturate beyond irradiation times of 28 hours. At this time, a linear shrinkage of 2.4% is calculated (El-Azab and Ghoniem, 1994), which is a few orders of magnitude larger than the helium and loop swelling components in the matrix during early irradiation. In presenting the results for Nicalon–SiC composite system, irradiation-induced dimensional changes in the fibers are represented by the shrinkage component only. The irradiation creep compliance is assumed similar to that of the matrix.

4. Total creep and relaxation functions

It has been experimentally found that irradiation creep, like diffusional creep, is linearly dependent on the applied stress for almost all nuclear structural materials. This also applies to SiC (Price, 1977). Thermal creep of CVD SiC is determined to be of the diffusional type, and well explained by the linear Nabarro–Harring diffusional creep relationship (Gulden and Driscoll, 1971). DiCarlo (1986) has experimentally found that the stress–strain relationship is linear for SCS-6 fibers. For Nicalon fibers, DiCarlo and Morscher (1991) have also found that the thermal creep rate is proportional to $\sigma^{1.2}$. In the present analysis, the stress exponent for thermal creep of Nicalon fibers is taken to be approximately unity, so that Nicalon fibers can be treated as a linear viscoelastic material.

By comparing the thermal creep data of CVD-SiC (Gulden and Driscoll, 1971) to those of SCS-6 and Nicalon fibers (DiCarlo and Morscher, 1991) it has been found that the thermal creep of CVD-SiC can be totally ignored below 1400°C (El-Azab and Ghoniem, 1994). The total creep compliance for the CVD-SiC matrix is composed of an elastic component and an irradiation component, as follows:

$$J_m(t) = \frac{1}{E_m} + K\phi t. \tag{15}$$

The relaxation modulus and the creep compliance are related by:

$$\int_0^t J_m(t-t')E_m(t')\,dt' = t, \tag{16}$$

and their Laplace transforms are therefore related by:

$$\hat{E}_m(s)\hat{J}_m(s) = \frac{1}{s^2}, \tag{17}$$

where s is the Laplace parameter. Using the relationship between the creep compliance and the relaxation modulus, the latter can be recovered as:

$$E_m(t) = E_m \exp(-K\phi E_m t). \tag{18}$$

Similar expressions are used for SCS-6 and Nicalon fibers in the absence of thermal creep.

By considering both thermal and irradiation creep, the total creep compliance for Nicalon fibers is written as:

$$J_f(t) = \frac{1}{E_f} + K\phi t + C_{NIC}(T)t^m, \tag{19}$$

where the last term is the thermal creep contribution, $m = 0.4$, and the subscripts "f" and "NIC" refer to the Nicalon fiber. $C_{NIC}(T)$ is a temperature-dependent function, which is given by (DiCarlo and Morscher, 1991):

$$C_{NIC}(T) = A_{NIC} \exp\left(-\frac{24200}{T}\right), \tag{20}$$

in which $A_{NIC} = 8.316$ for stresses in MPa, T in K and time in seconds. By taking the Laplace transform of Eq. (19) and using Eq. (17), the s-multiplied relaxation modulus for Nicalon fibers is obtained as:

$$s\hat{E}_f(s) = \frac{E_f}{1 + E_f K\phi s^{-1} + E_f C_{NIC}\Gamma(1+m)s^{-m}}, \tag{21}$$

where $\Gamma(1+m)$ is the gamma function.

There is no direct inversion formula for expression (21). However, a widely used approximate inversion method, which proved to be highly accurate for the purpose of obtaining time-dependent solutions in the theory of linear viscoelasticity, is used in the present work. This formula is due to Schapery (1962) . The statement of that inversion formula is as follows: if $\hat{\psi}(s)$ is the Laplace transform, which is known, for the function $\psi(t)$, then the latter is approximately given by:

$$\psi(t) \simeq \left[s\hat{\psi}(s)\right]_{s=0.5/t}. \tag{22}$$

While equation (22) is simple to use, it is found to be as accurate as other numerical techniques of inversion, such as the collocation method. Details of comparison of this method with exact and collocation techniques are found in (Schapery, 1962). This inversion method is used by Pipkin (1986) to invert Laplace transformed viscoelastic solutions. By applying Schapery's method, the relaxation modulus is then given in the time domain by:

$$E_f(t) = \frac{E_f}{1 + 2E_f K\phi t + 1.32 E_f C_{NIC}\Gamma(1+m)t^m}. \tag{23}$$

For SCS-6 fibers, the total transverse and axial creep compliances are written as:

$$J_{tr}(t) = \frac{1}{E_{tr}} + K\phi t + C_{SCS}(T)t^p,$$

$$J_{ax}(t) = \frac{1}{E_{ax}} + \frac{K\phi t}{(1-f_c)} + C_{SCS}(T)t^p, \tag{24}$$

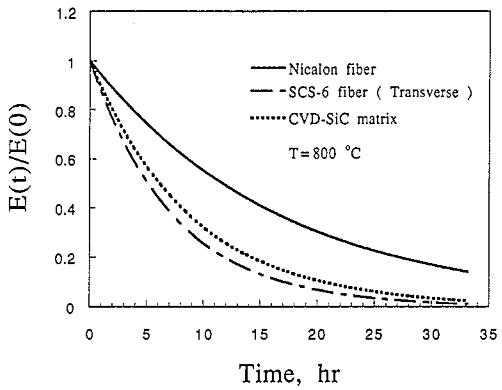

Fig. 2. Relaxation modulii at 800°C, showing the effect of irradiation creep only.

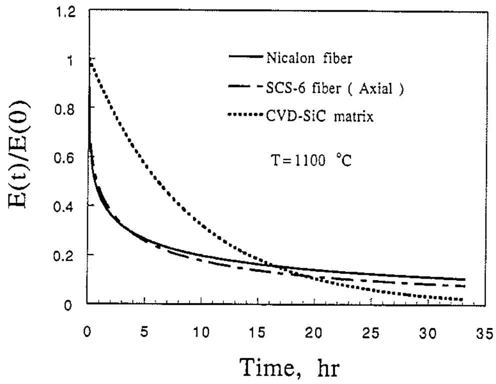

Fig. 3. Relaxation modulii at 1100°C. Both irradiation and thermal creep are considered.

where $p = 0.36$ and $C_{SCS}(T)$ is given by (DiCarlo and Morscher, 1991):

$$C_{SCS}(T) = A_{SCS} \exp\left(-\frac{25800}{T}\right), \tag{25}$$

in which $A_{SCS} = 13.112$ for stresses in MPa, T in K and time in seconds. The corresponding relaxation moduli are given by:

$$E_{tr}(t) = \frac{E_{tr}}{1 + 2E_{tr}K\phi t + 1.283 E_{tr} C_{SCS} \Gamma(1+p) t^p},$$
$$E_{ax}(t) = \frac{E_{ax}}{1 + 2E_{ax}\frac{K\phi t}{(1-f_c)} + 1.283 E_{ax} C_{SCS} \Gamma(1+p) t^p} \tag{26}$$

If the temperature is below thermal creep threshold, only irradiation creep will be considered and the fiber relaxation moduli will be given by a formula similar to Eq. (18), with E_m, being replaced by fiber elastic moduli. In treating the multi-axial stress state in fiber and matrix, uniaxial relaxation moduli are used. These moduli are shown in Figs. 2 and 3 for Nicalon fibers, SCS-6 fibers and CVD-SiC matrix.

5. Time-dependent solution

In obtaining the time-dependent solution, the elastic–viscoelastic correspondence principle is used. The time-dependent solution is first obtained for constant differential swelling strains (step input). The response, $\mathcal{R}(t)$, to an arbitrary differential swelling strain history is then obtained using a convolution integral of the form:

$$\mathcal{R}(t) = \int_{-\infty}^{t} R_{step}(t-t')\, d\Delta\epsilon^{s}_{tr,ax}(t') + \mathcal{H}(t)\Delta\epsilon_{th}, \tag{27}$$

where $\Delta\epsilon^{s}_{tr,ax}$ and $\Delta\epsilon_{th}$ are the differential swelling and thermal strains (defined later) and $R(t)$ and $\mathcal{H}(t)$ are functions of relaxation moduli. The developed elastic solution, which is given by Eqs. (6), can be used to obtain the Laplace transformed viscoelastic solution by replacing the elastic constants by their s-multiplied Laplace transforms. Mainly, $E_{tr} \to s\hat{E}_{tr}(s)$, $E_{ax} \to s\hat{E}_{ax}(s)$, $E_m \to s\hat{E}_m(s)$, $\nu_f \to s\hat{\nu}_f(s)$ and $\nu_m \to s\hat{\nu}_m(s)$. The quantities $a_{1,2}$ and $b_{1,2}$ given in Eq. (7) contain E_{tr}, E_{ax}, E_m, ν_f and ν_m. In the Laplace transformed viscoelastic solution, these quantities can be represented as functions of the Laplace parameter s as $\hat{a}_{1,2}(s)$ and $\hat{b}_{1,2}(s)$. The Laplace transformed solution is written as:

$$\hat{q} = \frac{s\hat{E}_{tr}\cdot s\hat{E}_m}{s}(1-f)\left(\frac{\hat{b}_2\Delta\hat{\epsilon}_{tr} - \hat{b}_1\Delta\hat{\epsilon}_{ax}}{\hat{a}_1\hat{b}_2 - \hat{a}_2\hat{b}_1}\right),$$
$$\hat{\sigma}^{f}_{z} = \frac{s\hat{E}_{tr}\cdot s\hat{E}_m}{s}(1-f)\left(\frac{-\hat{a}_2\Delta\hat{\epsilon}_{tr} + \hat{a}_1\Delta\hat{\epsilon}_{ax}}{\hat{a}_1\hat{b}_2 - \hat{a}_2\hat{b}_1}\right), \tag{28}$$

and the matrix stress is given by

$$\sigma^{m}_{z} = \left(\frac{-f}{1-f}\right)\sigma^{f}_{z}. \tag{29}$$

Application of Schapery's method to Eqs. (28) results in the time-dependent solution corresponding to constant differential mismatch strains. This solution is given by:

$$q(t) = E_{tr}(t)E_m(t)(1-f) \times \left(\frac{b_2(t)\Delta\epsilon_{tr} - b_1(t)\Delta\epsilon_{ax}}{a_1(t)b_2(t) - a_2(t)b_1(t)}\right),$$
$$\sigma_z^f(t) = E_{tr}(t)E_m(t)(1-f) \times \left(\frac{-a_2(t)\Delta\epsilon_{tr} + a_1(t)\Delta\epsilon_{ax}}{a_1(t)b_2(t) - a_2(t)b_1(t)}\right), \tag{30}$$

which is basically the elastic solution with the elastic constants and the mismatch strains being replaced by their time-dependent values. As defined by Pipkin (1986), this method of solution is known as the quasi-elastic approximation.

Since only differential swelling strains are considered in the convolution integral, it is convenient to rewrite the step solution in the form:

$$q(t) = [A_1(t) + B_1(t)]\,\Delta\epsilon_{th} + A_1\Delta\epsilon_{tr}^s + B_1\Delta\epsilon_{ax}^s,$$
$$\sigma_z^f(t) = [A_2(t) + B_2(t)]\,\Delta\epsilon_{th} + A_2\Delta\epsilon_{tr}^s + B_2\Delta\epsilon_{ax}^s, \tag{31}$$

where

$$\Delta\epsilon_{th} = \int_{T_0}^{T} \left[\alpha_m(T') - \alpha_f(T')\right]\,dT' \tag{32}$$

is the differential thermal mismatch. The quantities $\Delta\epsilon_{tr}^s = \epsilon_m^s - \epsilon_{tr}^s$ and $\Delta\epsilon_{ax}^s = \epsilon_m^s - \epsilon_{ax}^s$ are the transverse and axial differential swelling strains, respectively. Definitions of the other terms in (31) are given by:

$$A_1 = (1-f)E_{tr}(t)E_m(t) \times \left(\frac{b_2(t)}{a_1(t)b_2(t) - a_2(t)b_1(t)}\right),$$
$$B_1 = (1-f)E_{tr}(t)E_m(t) \times \left(\frac{-b_1(t)}{a_1(t)b_2(t) - a_2(t)b_1(t)}\right),$$
$$A_2 = (1-f)E_{tr}(t)E_m(t) \times \left(\frac{-a_2(t)}{a_1(t)b_2(t) - a_2(t)b_1(t)}\right),$$
$$B_2 = (1-f)E_{tr}(t)E_m(t) \times \left(\frac{a_1(t)}{a_1(t)b_2(t) - a_2(t)b_1(t)}\right). \tag{33}$$

By replacing $\Delta\epsilon_{tr}^s$ and $\Delta\epsilon_{ax}^s$ by the differentials $d\Delta\epsilon_{tr}^s(t')$ and $d\Delta\epsilon_{ax}^s(t')$ and implementing the convolution in (27), the viscoelastic solution due to arbitrarily varying differential swelling strains is given by:

$$q(t) = [A_1(t) + B_1(t)]\,\Delta\epsilon_{th} + \int_0^t A_1(t-t')\frac{d}{dt'}\Delta\epsilon_{tr}^s(t')\,dt' + \int_0^t B_1(t-t')\frac{d}{dt'}\Delta\epsilon_{ax}^s(t')\,dt',$$
$$\sigma_z^f(t) = [A_2(t) + B_2(t)]\,\Delta\epsilon_{th} + \int_0^t A_2(t-t')\frac{d}{dt'}\Delta\epsilon_{tr}^s(t')\,dt' + \int_0^t B_2(t-t')\frac{d}{dt'}\Delta\epsilon_{ax}^s(t')\,dt', \tag{34}$$

where zero initial differential swelling is considered.

6. Discussion of results

In the present work, the Poisson's ratios ν_f and ν_m are assumed constants. Under thermal creep conditions, the Poisson's ratios may not be constant. No experimental data is available for ν_f and ν_m under thermal or irradiation creep conditions. According to Golden and Graham (1988), the assumption of a constant Poisson's ratio in the range 0.35–0.41 is practical for most viscoelastic problems. However, experimental evidences have shown that Poisson's ratios under irradiation are of the order of ~0.45, which is considered in the present study (Kaae, 1977). The following elastic constants are used: E_m = 380 GPa for CVD-SiC matrix, and E_f = 420 GPa for SCS-6 fiber and 200 GPa for Nicalon fibers. Due to the data scatter in the thermal expansion coefficients, a thermal mismatch strain of −0.03% is used in all cases, which corresponds to a 300°C temperature cooling and $\alpha_m - \alpha_f$ =

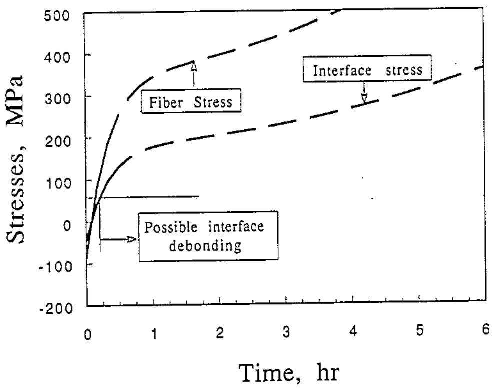

Fig. 4. Time evolution of internal stresses in the Nicalon–CVD SiC system at 900°C. Solid lines are for an interfacial failure stress limit of 60 MPa, while dashed lines are for the solution with the no-failure limit imposed.

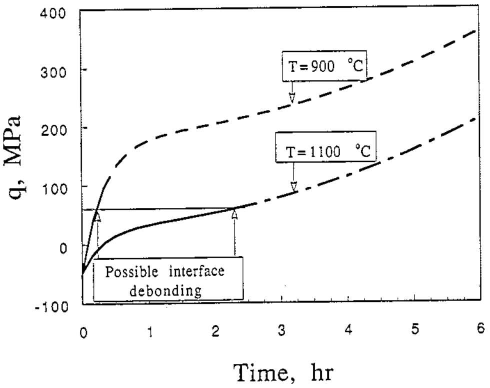

Fig. 5. Interface stress, q, in the Nicalon–CVD SiC system at 900 and 1100°C. Solid lines are for an interfacial failure stress limit of 60 MPa, while dashed lines are for the solution with the no-failure limit imposed.

10^{-6} K^{-1}. It will be shown later that this thermal mismatch component can be unimportant in optimizing SiC–SiC composites for fusion applications.

Fig. 4 shows the evolution of axial fiber and interface stresses in Nicalon–SiC composite system. The interface stress changes from compressive to tensile in the first few hours of operation. Also the axial fiber and matrix stress state reverses. This change is due to the fast fiber shrinkage under neutron irradiation. Fig. 5 shows the effect of temperature on the interface stress. At 1100 °C thermal creep is also operable, which yields relatively lower tensile stress at the fiber–matrix interface. Because of the fast Nicalon fiber shrinkage under irradiation, interface debonding is anticipated. Experimental studies (Sneed et al., 1992; Jones, 1994) have shown that Nicalon fibers, which are non-crystalline, *always* debonded from the CVD-SiC matrix upon irradiating the composite.

A possible way to avoid interface debonding in SiC–SiC composites under irradiation, is to start with fibers of high content of crystalline SiC. In this case fiber dimensional changes can be closer to that of the matrix, which can be accommodated by creep of fibers and matrix. As has been previously mentioned, this is the reason SCS-6 fibers are considered in the present analysis. For SCS-6 fibers–CVD SiC composites, the analysis will proceed with parametric representation of the transverse and axial differential swelling in terms of the matrix swelling as follows:

$$\Delta\epsilon^s_{tr} = \epsilon^s_m - \epsilon^s_{tr} = c_{tr}\epsilon^s_m,$$

$$\Delta\epsilon^s_{ax} = \epsilon^s_m - \epsilon^s_{ax} = c_{ax}\epsilon^s_m, \tag{35}$$

where c_{tr} and c_{ax} will be called the differential swelling parameters. Obviously, these parameters depend, primarily, on the difference in composition between fibers and matrix. In particular, these composition differences are significant from the helium swelling point of view. Design limits of these two parameters must be established so that relative compositions can be tailored for *prospective* SiC fibers for fusion applications. In addition to c_{tr} and c_{ax}, the irradiation creep constant, K, is also varied between the fission and fusion limits to show its effect on the build-up and relaxation of mismatch stresses.

Two time scales are considered. The short-term re-

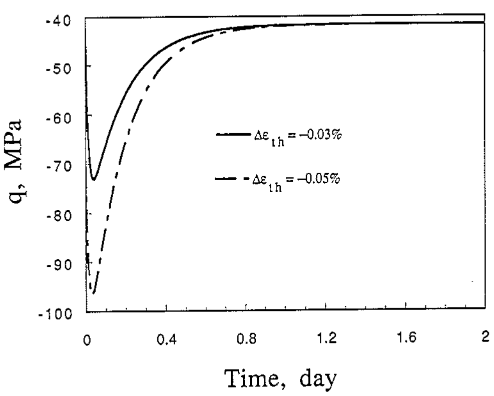

Fig. 6. Effect of initial thermal misfit strain on interface stress, q, for SCS-6-CVD SiC system in the loop swelling regime. ($K = 10^{-25}$ (MPa (n·cm^{-2}) s)$^{-1}$, $T = 900$°C, $c_{tr} = c_{ax} = -0.2$.

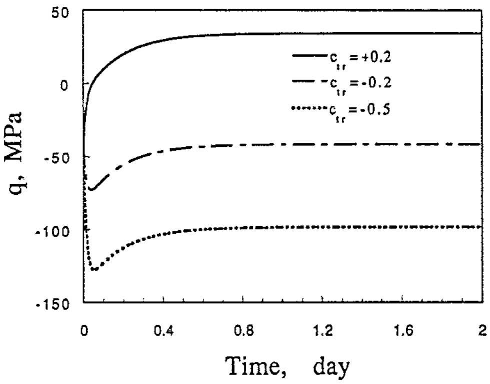

Fig. 7. Effect of c_{tr} on the early evolution of interface stress, q, for the SCS-6-CVD SiC system. ($K = 10^{-25}$ (MPa (n·cm^{-2}) s)$^{-1}$, $T = 900°$C, $c_{ax} = -0.2$.

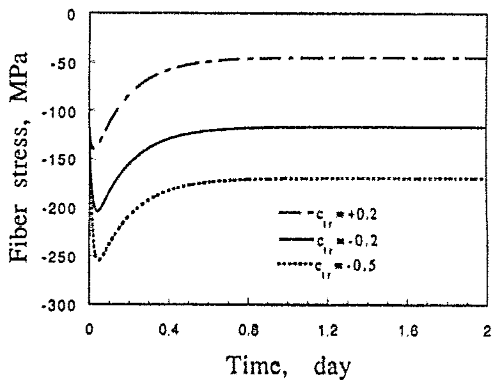

Fig. 8. Effect of c_{tr} on the early evolution of fiber stress, σ_z^f, for the SCS-6-CVD SiC system. ($K = 10^{-25}$ (MPa n·cm^{-2} s)$^{-1}$, $T = 900°$C, $c_{ax} = -0.2$.

laxation which occurs over a few days and includes the relaxation of initial thermal mismatch and loop swelling. Long-term relaxation, on the other hand, is governed by a balance between swelling and creep rates. The effect of initial thermal mismatch is shown in Fig. 6. This component dies away in time due to creep, and the final trends in mismatch stresses are mainly determined by creep and the long-term helium differential swelling.

Figs. 7 and 8 show the effect of the differential swelling parameter c_{tr} on the interface stress and fiber axial stress, respectively. A compressive interface stress is desired in ceramic composites with weak interfaces. The interface stress can be maintained compressive if the fiber swelling is kept higher than that of the matrix, which corresponds to negative values of c_{tr}. The interface stress controls the process of fiber debonding and frictional sliding at composite failure, while the axial fiber stress is important in determining matrix crack initiation and fiber bridging. It is noted that the matrix fractures easily at high compressive fiber stresses, which is likely to occur at higher fiber swelling rates. Thus, spontaneous matrix fracture can be possible under irradiation. Therefore, different controlling factors must be carefully explored. Since swelling depends on the irradiation temperature, significant stress differences between different temperature zones in the reactor structure are expected. Figs. 9 and 10 show the effect of irradiation temperature on the interface stress and the axial matrix stress, respectively. During early irradiation, where loop swelling rate is significant, these stresses increase.

The effect of irradiation creep constant, K, on the relaxation process is shown in Figs. 11 through 14. Lower values of K may be desirable, which result in slower short-term stress relaxation (Figs. 11 and 12). However, during helium swelling mode (Figs. 13 and 14), the differential swelling parameters, c_{tr} and c_{ax} and the irradiation creep constant, K, determine the mismatch stress state. As shown in Figs. 13 and 14, total recovery of mismatch stresses may be possible in 2–3 years, depending on the value of K, the parameters c_{tr} and c_{ax} and the operating temperature.

It is well established that mismatch stresses are important in determining the fracture strength and toughness of ceramic matrix composites. Approximate expressions for the matrix cracking stress, σ_c, and the ultimate tensile strength, σ_u, for ceramic matrix composites are given by (Evans, 1990, 1991):

$$\sigma_c = \left[\frac{6\tau\Gamma_m f^2 E_f E^2}{(1-f)E_m^2 R_f}\right]^{1/3} - \sigma_z^m\left(\frac{E}{E_m}\right),$$

$$\sigma_u = fS_b + (1-f)\left[S_m - \sigma_m^z\right], \qquad (36)$$

where τ is the frictional stress at the interface, Γ_m is the fracture energy for matrix, E is the composite modulus, S_b is the fiber bundle strength, and S_m is the matrix flaw stress. From the present study, it is clear that σ_0 and σ_u are time dependent since σ_m^z and τ vary significantly with time (τ depends on the interface pressure). The toughness of the composite depends strongly on the frictional energy dissipation during fiber pull-out and fiber bridging of crack tips. These

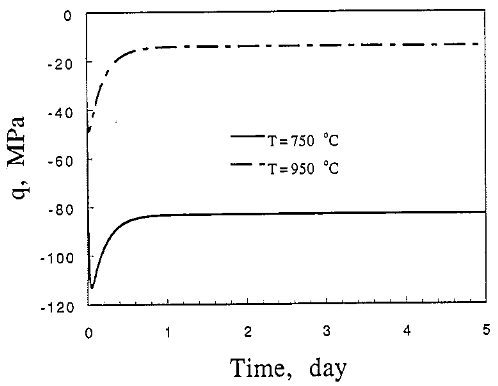

Fig. 9. Effect of temperature on the early evolution of interface stress, q, for the SCS-6-CVD SiC system. ($K = 10^{-25}$ (MPa n·cm^{-2}s)$^{-1}$, $c_{tr} = c_{ax} = -0.2$.

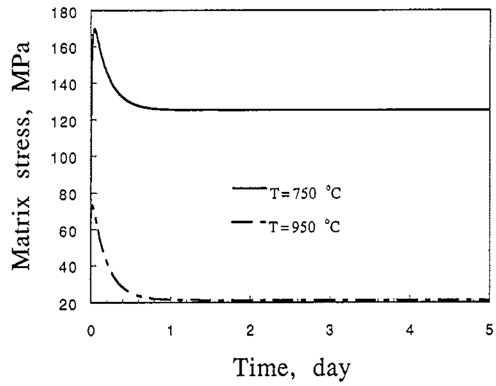

Fig. 10. Effect of temperature on the early evolution of matrix stress, σ_z^m, for the SCS-6-CVD SiC system. ($K = 10^{-25}$ (MPa n·cm^{-2}s)$^{-1}$, $c_{tr} = c_{ax} = -0.2$.

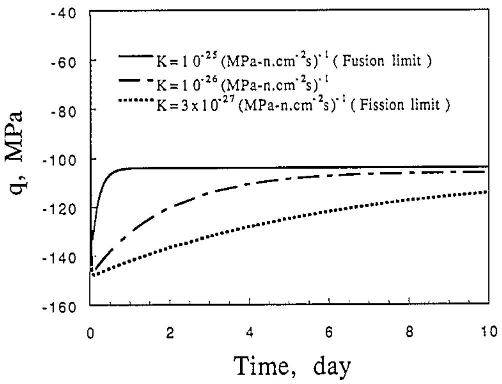

Fig. 11. Effect of the irradiation creep constant on the early evolution of interface stress, q, for the SCS-6-CVD SiC system. (T = 800°C, $c_{tr} = c_{ax} = -0.3$.

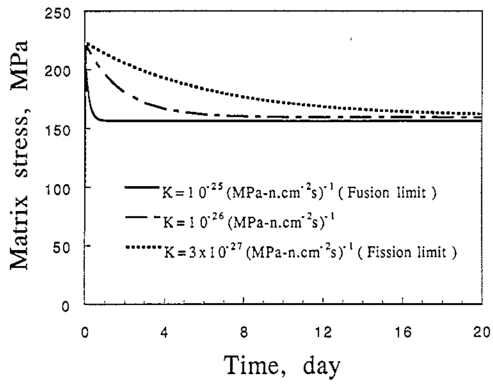

Fig. 12. Effect of the irradiation creep constant on the early evolution of matrix stress, σ_z^m, for the SCS-6-CVD SiC system. (T = 800°C, $c_{tr} = c_{ax} = -0.3$.

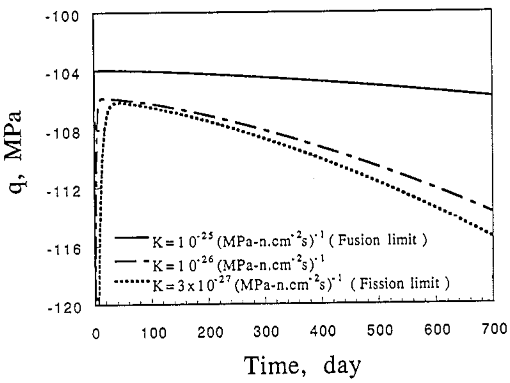

Fig. 13. Effect of the irradiation creep constant on the recovery of interface stress, q, for the SCS-6-CVD SiC system in the helium swelling regime. (T = 800°C, $c_{tr} = c_{ax} = -0.3$.

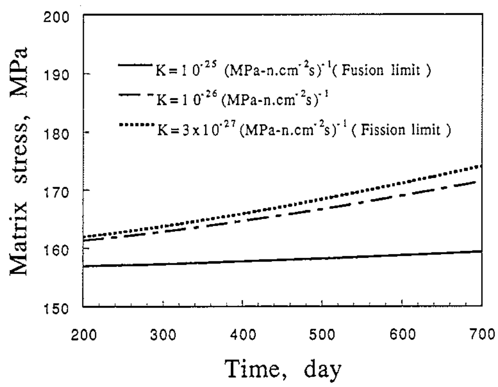

Fig. 14. Effect of the irradiation creep constant on the recovery of matrix stress, σ_z^m, for the SCS-6-CVD SiC system in the helium swelling regime. (T = 800°C, $c_{tr} = c_{ax} = -0.3$.

processes depend on interfacial friction characteristics and on the fiber stress.

7. Conclusions

The complex nature of in-service behavior of SiC–SiC composite structures under fusion neutron irradiation conditions makes it imperative to consider novel processing optimization techniques. Development of time-dependent strain components results in build-up/relaxation characteristics of interfacial pressure, fiber and matrix stresses. The study, *even though partially parametric*, underscores the need to avoid early loss of in-service strength by appropriate processing. The following conclusions can be drawn from the present analysis:

(i) The initial thermal mismatch stresses are completely relaxed in a relatively short time (within few days) in a fusion environment. Significant composite strength changes are anticipated due to this relaxation process. Different techniques for optimizing the mechanical properties of structural composite for fusion must therefore be explored.

(ii) Since both loop and helium swelling are temperature-dependent, the operating temperature is shown to influence the composite fracture strength and toughness.

(iii) Mismatch stresses in SiC–SiC composites under fusion conditions are ultimately controlled by the balance between fiber/matrix differential helium swelling and irradiation creep. The former is sensitive to compositions and can be used to control the state of mismatch stresses for optimum structural properties.

(iv) Reinforcement of a SiC matrix with Nicalon-type fiber is shown to result in significant loss of strength (debonding) in a matter of hours under fusion neutron irradiation. This behavior is borne out in recent fission-reactor irradiation experiments, though on a longer time scale (Jones, 1994).

(v) The lack of irradiation-induced shrinkage in SCS-6 type fibers, *which is considered in the present study to represent an irradiation resistant fiber*, may allow the possibility of matrix toughening by fibers of high initial content of crystalline SiC to persist under irradiation.

(vi) One of the parameters identified in this study is the transverse fiber–matrix differential swelling fraction, c_{tr}. This fraction is defined as the ratio of the differential fiber–matrix swelling to the matrix swelling, as given by Eq. (35). This fraction may be controlled by boron doping for excess helium production, or by having a graphite core in the fiber.

(vii) Conclusions of this analysis are obviously dependent on the accuracy of the data base. Although inelastic deformation of SiC under fission neutron irradiation is well documented, the accuracy of our proposed extrapolation to fusion conditions should be calibrated with direct experiments, once a fusion neutron test facility is constructed.

(viii) Since relaxation of initial thermal mismatch stresses occurs after low fluence neutron exposure, experimental tests can be devised to explore this behavior with low fluence irradiation test facilities.

(ix) It is to be noted that in a complete analysis of the problem, external loading effects will have to be considered.

References

Aveston, J., G.A. Cooper and A. Kelly (1971), Single and multiple fracture, in: *The Properties of Fiber Composites* (Conference Proceedings), National Physical Laboratory, IPC Science and Technology Press Ltd., pp. 15-26.

Aveston, J. and A. Kelly (1973), Theory of multiple fracture of fibrous composites, *J. Mater. Sci. 8*, 352.

Budiansky, B., J.W. Hutchinson and A.G. Evans (1986), Matrix fracture in fiber-reinforced ceramics, *J. Mech. Phys. Solids 34* [2], 167.

Najmabadi, F. and the ARIES Team (1994), The ARIES II and ARIES IV Second Stability Tokamak Reactor Study: Final Report, UCLA-PPG 1461, in press.

DiCarlo, J.A. (1986), Creep of chemically vapor deposited SiC fibers, *J. Mater. Sci. 21*, 217.

DiCarlo, J.A. and G.N. Morscher (1991), Creep and stress relaxation modeling of polycrystalline ceramic fibers, in: *Failure Mechanisms of High Temperature Composite Materials*, AD-Vol. 22, AMD-Vol. 122, ASME, pp. 15–22.

El-Azab, A. and N.M. Ghoniem (1994), Phenomenological inelastic constitutive equations for SiC and SiC fibers under irradiation, *Fusion Technol. 26*, 1250.

Evans, A.G. (1990), The mechanical behavior of ceramic composites, in: *Modelling of Material Behavior and Design*, eds. J.D. Embury and A.W. Thompson, TMS Publication, pp. 245–267.

Evans, A.G. (1991), The mechanical properties of fiber-reinforced ceramic, metal and intermetallic matrix composites, in: *High Performance Composites for the 1990's*, Proc. TMS Northeast Regional Symposium sponsored by TMS-New Jersey Chapter, Morristown, New Jersey, June 6–8, 1990, eds. S.K. Das, C.P. Ballard and F. Marikar, TMS Publication, pp. 1–29.

Gao, Yu-Chen, Yiu-Wing Mai and B. Cotterell (1988), Fracture of fiber-reinforced materials *J. Appl. Math. Phys. (ZAMP) 39*, 550.

Golden, J.M. and G.A.C. Graham (1988), *Boundary Value Problems in Linear Viscoelasticity*, Springer, Berlin.

Gulden, T.D. and C.F. Driscoll (1971), *Creep of Chemically Vapor-Deposited β-SiC with an Analysis of Creep in Bending*, Gulf General Atomic Co., GA-10366.

Hutchinson, J.W. and H.M. Jensen (1990), Models for fiber debonding and pullout in brittle composites with friction, *Mech. Mater. 9*, 139.

Jones, R. (1994), SiC–SiC Composite Development for Fusion Structural Applications, presented in: *The US–Japan Workshop on Power Reactor Studies*, March 14–17, University of California, San Diego, USA.

Kaae, J.L. (1977), The mechanical behavior of biso-coated fuel particles during irradiation, Part I: Analysis of stresses and strains generated in the coating of a biso fuel particle during irradiation, *Nucl. Technol. 35*, 359.

Kelly, A. and K.N. Street (1972a), Creep of discontinuous fiber composites, I. Experimental behavior of lead–phosphor bronze, *Proc. R. Soc. Lond. A 328*, 267.

Kelly, A. and K.N. Street (1972b), Creep of discontinuous fiber composites, II. Theory for the steady-state, *Proc. R. Soc. Lond. A 328*, 283.

Liang, C. and J.W. Hutchinson (1993), Mechanics of the fiber pushout test, *Mech. Mater. 14*, 207.

Okamura, K., M. Matsuzawa, M. Sato, Y. Higashiguchi and S. Morozumi (1985), Effects of neutron irradiation on SiC fibers, *J. Nucl. Mater. 133–134*, 705.

Pachalis, J.R., Jin Kim and Tsu-Wei Chou (1990), Modeling of creep of aligned short-fiber reinforced ceramic composites, *Compos. Sci. Technol. 37*, 329.

Pipkin, A.C. (1986), *Lectures on Viscoelasticity Theory*, Springer, Berlin.

Price, R.J. (1973), Neutron irradiation-induced voids in β-Silicon Carbide, *J. Nucl. Mater. 48*, 47.

Price, R.J. (1977), Properties of silicon carbide for nuclear fuel particle coatings, *Nucl. Technol. 35*, 320.

Schapery, R.A. (1962), Approximate methods of transform inversion for viscoelastic stress analysis, in: *Proceedings of the Fourth U.S. National Congress on Applied Mechanics*, ASME Publications, pp. 1075–1085.

Sigl, L.S. and A.G. Evans (1989), Effects of residual stresses and frictional sliding on cracking and pull-out in brittle matrix composites, *Mech. Mater. 8*, 1.

Sneed, L.L., D. Steiner and S.J. Zinkle (1992), Measurement of the effect of radiation damage to ceramic composite interfacial strength, *J. Nucl. Mater. 191–194*, 566.